An experimental and theoretical study of the molecular structure and vibrational spectra of iodotrimethylsilane ($SiIMe_3$)†

Manuel Montejo,[a] Sarah L. Hinchley,[b] A. Ben Altabef,[cd] Heather E. Robertson,[b] Francisco Partal Ureña,[a] David W. H. Rankin*[b] and Juan J. López González*[a]

Received 29th July 2005, Accepted 11th October 2005
First published as an Advance Article on the web 8th November 2005
DOI: 10.1039/b510827f

The gas-phase molecular structure of iodotrimethylsilane (ITMS) has been determined from electron diffraction data. Infrared and Raman spectra have been completely assigned. The experimental work is supported by *ab initio* HF and MP2 calculations for the gas-phase structure determination and DFT(B3LYP) calculations, combined with Pulay's SQM method, for the vibrational spectra data.

Introduction

Alkylsilylhalides play an important role as precursors of silanols, which are well-known intermediate products in sol-gel processes and are commonly used for the production of ceramics, glasses, fibres, *etc*.[1] In addition, trimethylsilylhalides, and specifically iodotrimethylsilane, are widely used in organic and organometallic reactions as cleavage reagents, catalysts or silation agents, among others.[2–8] Studies of the molecular structures and vibrational spectra of the chemical species of the Me_3SiX (X = H, F, Cl, Br or OMe) series were performed recently.[9–11] These studies allowed the authors to reach a complete description of the theoretical molecular structures, in agreement with the experimental data already in the literature. Moreover, supported by both theoretical and experimental data, a unified explanation of the main features observed in the vibrational spectra of the whole family was proposed.

For the iodo-derivative of the series [iodotrimethylsilane (ITMS)] only one paper related to the study of its molecular structure[12] and two dealing with the analysis of its vibrational spectra[13,14] are present in the literature. The geometry of ITMS has not been widely reported, for example, Rexroad *et al*.[12] carried out a study of ITMS by microwave spectroscopy. However, only one geometric parameter was reported, namely the Si–I distance [246(2) pm], whilst other parameters were held at fixed values. Goubeau and Sommer[13] recorded the Raman spectrum of the liquid phase and proposed the existence of appreciable double bond character between Si and I in ITMS. This was proposed from comparison of the calculated value for the force constant associated with the Si–I bond stretching (from the Raman spectrum data, 2.10 mdyn $Å^{-2}$) and that corresponding to a single bond Si–I from the theory (1.58 mdyn $Å^{-2}$). The slight increase of the dipole moment (μ = 2.46 D) when going from the bromine to the iodine compound in the series Me_3SiX (for X = Cl, Br, I) also supported this interpretation.

Later, Bürger reported the IR spectra of the gas and liquid (far region) phases of ITMS.[14] A detailed study of the PQR shape of the band associated with ν_s SiC_3, using the Raman data from ref. 13, was performed, and a normal mode analysis for the low-frequency fundamentals [those corresponding to skeletal C_3SiX modes (torsion modes excluded)] was carried out. Bürger proposed an incomplete assignment of the experimental bands to the fundamental normal modes of ITMS, which was compared with those for the rest of the halogen derivatives in the series.

In this paper, we report a more complete and accurate molecular structure for ITMS and an improved vibrational assignment for this molecule. We have combined gas-phase electron diffraction (GED) and quantum mechanical calculations to obtain reliable molecular structure data, and have combined newly recorded IR (gas and liquid phase) and Raman (liquid phase) data with results of theoretical calculations, including the SQMFF methodology, in order to corroborate the original assignments. Furthermore, the results of the vibrational study of the title molecule, along with those previously obtained for the rest of the trimethylsilylhalide series,[10,11] allow us to give a unified description of the experimental features observed for the whole family of compounds.

Experimental methods

Commercial iodotrimethylsilane samples (>99%) were purchased from Sigma-Aldrich and used without further purification.

Gas electron diffraction (GED)

Data were collected for ITMS using the Edinburgh gas-phase electron diffraction apparatus.[15] An accelerating voltage of around 40 kV was used, representing an electron wavelength

[a] *Departmento de Química Física y Analítica, Facultad de Ciencias Experimentales, Universidad de Jaén, Campus Universitario Las Lagunillas, Edif. B-3, 23071 Jaén, Spain. E-mail: jjlopez@ujaen.es*
[b] *School of Chemistry, University of Edinburgh, West Mains Road, Edinburgh, UK EH9 3JJ. E-mail: d.w.h.rankin@ed.ac.uk*
[c] *Instituto de Química Física, Facultad de Bioquímica, Química y Farmacia, Universidad Nacional de Tucumán, San Lorenzo 456, 4000 Tucumán, R. Argentina*
[d] *Member of the Carrera del Investigador Científico, CONICET, R. Argentina*

† Electronic supplementary information (ESI) available: Tables S1–S7 and Figs. S1 and S2. See DOI: 10.1039/b510827f

Table 1 Nozzle-to-plate distances (mm), weighting functions (nm^{-1}), correlation parameters, scale factors and electron wavelengths (pm) used in the electron-diffraction study

Nozzle-plate distance[a]	130.44	290.81
Δs	2	1
s_{min}	70	20
sw_1	80	40
sw_2	258	112
s_{max}	300	130
Correlation parameter	0.2888	0.4540
Scale factor[b]	0.788(8)	0.747(6)
Electron wavelength	6.1282	6.1282

[a] Determined by reference to the scattering pattern of benzene vapour. [b] Values in parentheses are the estimated standard deviations.

of approximately 6.0 pm. Scattering intensities were recorded on Kodak Electron Image films at nozzle-to-film distances of 130.44 and 90.81 mm with sample and nozzle temperatures held at 293 K. The weighting points for the off-diagonal weight matrices, correlation parameters and scale factors for both camera distances for ITMS are given in Table 1. Also included are the electron wavelengths as determined from the scattering patterns for benzene, which were recorded immediately after the patterns for the sample compounds. The scattering intensities were measured using an Epson Expression 1600 Pro Flatbed Scanner and converted to mean optical densities as a function of the scattering variable, s, using an established program.[16] The data reduction and the least-squares refinement processes were carried out using the ed@ed program[17] employing the scattering factors of Ross *et al.*[18]

IR and Raman spectra

IR spectra were recorded in the 400–4000 cm^{-1} range for ITMS in the liquid and gaseous phases with an FT-IR Bruker Tensor 27 spectrophotometer, equipped with a Globar source and a DTGS detector, using standard cells for liquid and gas (10 cm path length) both equipped with CsI windows. All the spectra were obtained with a resolution of 1.0 cm^{-1} and 50 scans.

The Raman spectrum in the liquid phase was recorded with a Bruker RF100/S FT-Raman spectrometer, equipped with a Nd:YAG laser (excitation line 1064 nm, 600 mW of laser power) and a cooled Ge detector at liquid nitrogen temperature, using a standard liquid cell. The spectrum was recorded with a resolution of 1.0 cm^{-1} and 100 scans.

Computational methods

Geometry optimisations

Calculations were performed with the resources of the EPSRC National Service for Computational Chemistry Software (NSCCS) using Gaussian 03.[19] All MP2 calculations were frozen core [MP2(fc)]. Geometry optimisations for ITMS were performed in C_{3v} and C_s symmetry. There are two possible orientations of the methyl groups relative to the Si–I bond that allow the molecule to possess C_{3v} symmetry, eclipsed and staggered, *i.e.* when ϕH(4/9/12)–C(3/7/11)–Si(1)–I(2) = 0° or 180°. The two C_s structures can have either two groups staggered and one eclipsed or two eclipsed and one staggered. Low-level calculations on these four conformers were performed using HF theory[20] with a 3-21G* basis set[21] on all atoms. It was observed that when three H atoms eclipse the Si–I bond (ϕH–C–Si–I = 0°), three imaginary frequencies were returned [198i cm^{-1} (A_2) and 183i cm^{-1} (E)]. When two H atoms eclipse the Si–I bond and one is staggered (C_s), two imaginary frequencies were returned [179.0i cm^{-1} (A″) and 169.6i cm^{-1} (A′)]. Changing this to one eclipsed and two staggered groups (C_s) resulted in only one imaginary frequency [162.9i cm^{-1} (A″)]. All the lowest-lying frequencies relate to the torsions of the methyl groups relative to the Si–I bond. When all torsion angles were changed from 0 to 180°, a C_{3v} structure, all frequencies were real.

One of the C_s conformers (ϕH–C–Si–I = 0, 180 and 180°) is a transition state on the potential energy surface, with the barrier to methyl rotation lying ~7 kJ mol^{-1} above the ground state structure. The remaining structures are ~14 and ~23 kJ mol^{-1} above the ground-state energy. This even spacing implies that the rotations of the methyl groups relative to the Si–I bond are independent motions, and that there is no steric crowding influencing their movement. The energies and observed frequencies are summarised in Table S1.†

All further discussion relates to the global minimum structure of ITMS (C_{3v} symmetry). Beyond a 3-21G* basis set, the next Pople-style basis set available for iodine is 6-311G*.[22a] Other than this, iodine has to be treated specially using a basis set that possesses an effective core potential (ECP). The use of the SDB-cc-pVTZ basis set and ECP was investigated for iodine,[23] whilst the standard 6-31G*[24] and 6-311+G*[22b] basis sets were used for H, C and Si with the MP2[25] level of theory.

Analytic second derivatives of the energy with respect to the nuclear coordinates calculated at the HF level with the SDB-cc-pVTZ (I) and 6-31G* (H, C and Si) basis sets gave a force field which was then used to provide estimates of the amplitudes of vibration (u) for use in the GED refinements. This force field was also used to calculate the vibrational frequencies, which provide the information about the nature of the stationary point. As described above, a lower-level force field (HF/3-21G*) was used initially to probe the potential energy surface of ITMS to locate real minima. Calculations on the related H-, F-, Cl- and Br-trimethylsilanes were also performed in the range from HF/3-21G* to MP2/6-311G**. The results of the highest-level *ab initio* calculations for $SiMe_3X$ (X = H, F, Cl, Br or I) are reported in Table 2, whilst the results from the lower levels can be found in the supporting information (Table S3).† The molecular structure of ITMS with atom numbering is shown in Fig. 1.

Vibrational spectra

Theoretical calculations of the IR and Raman vibrational spectra were performed with Gaussian 03.[19] The hybrid B3LYP functional[26,27] was used with the Pople-style 6-311G**[22a] basis set. As for the geometry optimisations, an ECP was required for the definition of the iodine atom. In this case, two potentials, LanL2DZ[28] and LanL2DZdp,[28,29] were investigated.

The force-constant matrices obtained at this level of calculation, expressed in Cartesian coordinates, were used to build a

Table 2 Geometric parameters for $SiMe_3X$ (X = H, F, Cl, Br and I) at the MP2(fc) level with the 6-311G** basis set. For X = I, the SDB-cc-pVTZ basis set and ECP was also applied to iodine, with the 6-311+G* basis applied to all other atoms[ab]

Parameter	X = H	X = F	X = Cl	X = Br	X = I[c]	X = I[d]
*r*C–Hα	109.5	109.5	109.5	109.6	109.6	109.6
*r*C–Hβ	109.4	109.4	109.4	109.4	109.3	109.3
*r*Si–C	188.0	186.4	186.5	186.7	186.8	187.0
*r*Si–X	148.6	163.3	208.1	225.4	249.9	248.5
∠Si–C–Hα	110.9	110.6	110.3	110.1	109.8	110.3
∠Si–C–Hβ	111.3	111.3	111.1	111.1	111.1	111.3
∠Hα–C–Hβ	107.7	107.8	108.1	108.2	108.2	108.0
∠Hβ–C–Hβ	107.8	107.9	108.1	108.2	108.2	108.0
∠C–Si–C	110.2	110.4	111.5	111.4	111.4	111.6
∠X–Si–C	108.8	107.5	107.3	107.4	107.5	107.3
Energy[e]	−408.9981	−508.1528	−868.1142	−2980.9621	−7325.4830	−419.7307

[a] All bond lengths in pm, all angles in °. [b] See Fig. 1 for atom numbering and definition of α and β hydrogen atoms. [c] 6-311G** basis set used on all atoms. [d] 6-311+G* on H, C and Si, SDB-cc-pVTZ on I. [e] Absolute energies in Hartrees.

force-constant matrix expressed in a set of natural coordinates as described in Table S2.† This was done for a better interpretation of the potential energy distribution matrix (PEDM) and to perform a normal-mode analysis, including the application of the SQMFF methodology. These natural coordinates and the set of scale factors associated with them have been defined as proposed by Fogarasi *et al.*[30]

The MOLVIB program[31,32] was used for the normal-mode analysis, the scaling of the force field using the Pulay's method,[33] and to refine the scale factors. The scale-factor refinement was performed by closely fitting the theoretical vibrational frequencies to those obtained experimentally, using a root-mean-squares procedure.

Results

Geometry optimisations

The molecular structures of a series of related molecules have been studied at the MP2(fc)/6-311G** level. All the molecules have the general structure $SiMe_3X$, where X is H(TMS), F(FTMS), Cl(CTMS), Br(BTMS) or I(ITMS). The main molecule of interest for the research reported in this paper is iodotrimethylsilane (ITMS). This also presented an interesting challenge for theory, as iodine has very few all-electron basis sets available, so the opportunity was taken to evaluate the performance of a pseudopotential. Initially, as reported in the Experimental section, a search of the potential-energy surface (PES) of ITMS was performed to probe the orientation of the methyl groups relative to the Si–I bond. Four stationary points were observed, when ϕH(4/9/12)–C(3/7/11)–Si(1)–I(2) = 0 or 180°, two possessing C_{3v} symmetry and two with C_s symmetry. When ϕHCSiI = 0, 180 and 180°, one imaginary frequency was returned, relating to rotation of one methyl group. At the lowest level of investigation (RHF/3-21G*) this transition state was predicted to be 7.1 kJ mol^{-1} above the ground state structure. Whilst the *absolute* energies of both structures would be expected to reduce with increased sophistication of calculation, previous experience indicates that the *relative* energies should change little, maintaining this barrier to rotation.

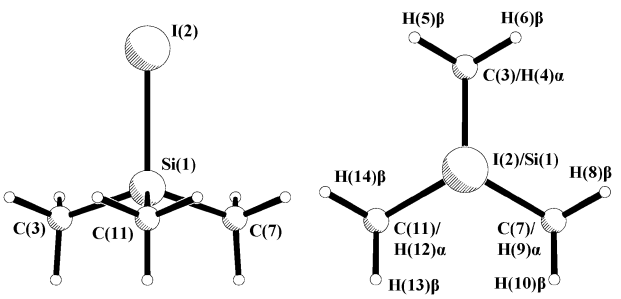

Fig. 1 C_{3v} molecular structure of ITMS showing the atom numbering scheme and (right) a perspective view down the I–Si bond.

The imaginary frequency returned for the transition state structure was large [163*i* cm^{-1} (A″], and the three lowest-lying frequencies for the ground-state structure were similarly large [162 cm^{-1} (A_2) and 166 cm^{-1} (E)]. The choice of C_{3v} symmetry for the GED model can thus be justified. If the values were a lot smaller, a choice of C_3 symmetry would have been more appropriate to allow for more vibrational motion at a higher temperature.

Two different types of basis set were used for iodine at the highest level of calculation [MP2(fc)]. First, the all-electron 6-311G*(*) was used in combination with 6-311G** on all other atoms. Secondly, the SDB-cc-pVTZ basis set with effective core potential (ECP) was used with 6-311+G* on all other atoms. The results from these calculations are presented in Table 2. It can be seen that the only parameter to be really affected by the choice of basis set is the Si–I distance. All other parameters are within 0.2 pm or 0.5° of one another. The Si–I distance is returned as 249.9 pm for the 6-311G** basis set, whilst the use of SDB-cc-pVTZ in combination with 6-311+G* returned an Si–I distance of 248.5 pm. This value should be well defined in the GED experiment, and comparison with the experimental results can aid our understanding of the accuracy of the calculations.

Gas electron diffraction (GED) refinement

On the basis of the *ab initio* calculations described above, electron-diffraction refinements were carried out using models with overall C_3 and C_{3v} symmetry to describe the gaseous structure. The C_3 structure was tested and it was found that it reverted to the C_{3v} structure, indicating that this is the

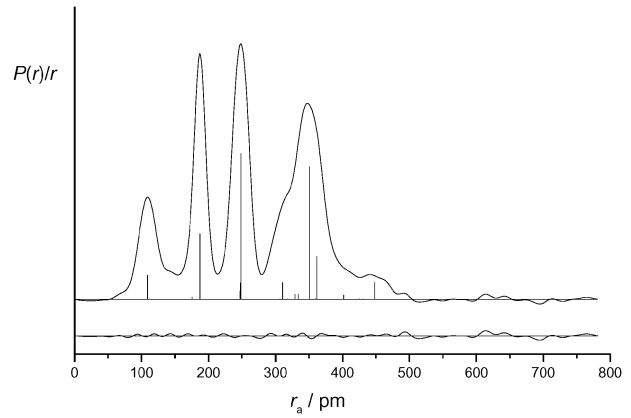

Fig. 2 Experimental and difference (experimental–theoretical) radial distribution curves, $P(r)/r$, for ITMS. Before Fourier inversion the data were multiplied by $s\exp(-0.000\,02s^2)/(Z_I - f_I)(Z_C - f_C)$.

preferred structure. The following model description refers to the C_{3v} structure only. The structure was defined in terms of six independent parameters (see Fig. 1 for atom numbering), comprising three bond lengths, two bond angles and a tilt of the methyl groups. The bond lengths were rC–H(p_1), rSi–C(p_2) and rSi–I(p_3). A single, average, rC–H value was used because the individual *ab initio* values differed by no more than 0.3 pm. The model also required two angle parameters, ∠Si–C–H(p_4) and ∠I–Si–C(p_5). The methyl tilt parameter was also included and a positive tilt indicated a decrease of the unique ∠Si–C–H and an increase of the symmetry-related ∠Si–C–H, *i.e.* away from the Si–I bond. The starting parameters for the r_{h1} refinement[34] were taken from the theoretical geometry optimised at the MP2(fc)/6-311+G*//SDB-cc-pVTZ level. A theoretical (RHF/6-31G*//SDB-cc-pVTZ) Cartesian force field was obtained and converted into a force field described by a set of symmetry coordinates using the program SHRINK.[34] From this, the RMS amplitudes of vibration (u_{h1}) and the perpendicular distance corrections (k_{h1}) were generated at the harmonic first-order curvilinear motion approximation. All geometric parameters and seven groups of amplitudes of vibration were then refined using the SARACEN method,[35] with flexible restraints employed for one parameter value and two amplitudes of vibration.

The final refinement for ITMS provided a good fit to the data, with $R_G = 0.079$ ($R_D = 0.047$), and can be assessed on the basis of the radial-distribution curve (Fig. 2) and the molecular-scattering intensity curves (Fig. S1).† Final refined parameters are listed in Table 3. The interatomic distances and corresponding RMS amplitudes of vibration are given in Table S4. The least-squares correlation matrix is given in Table S5 and the coordinates of the final refined structure from the GED investigation are given in Table S6.†

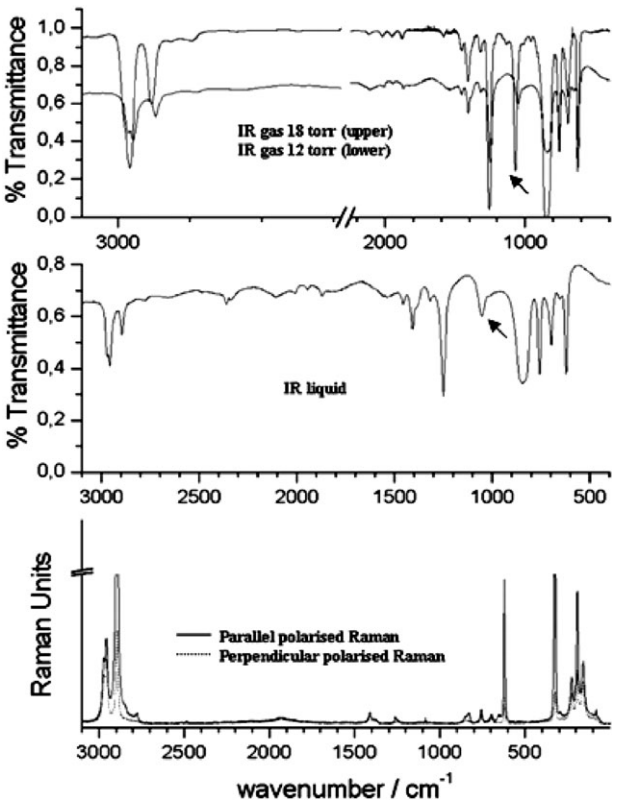

Fig. 3 Experimental IR (gas-phase) (top), experimental IR (liquid-phase) (middle) and experimental Raman (liquid-phase) (bottom) spectra. Bands due to hexamethyldisyloxane (see text) are marked with arrows.

Vibrational study

ITMS has C_{3v} geometry and its normal modes belong to symmetry species as follows: $8A_1 + 4A_2 + 12E$. Vibrations belonging to A_1 and E irreducible representations are active in both the IR and Raman spectra while the A_2 modes are inactive in both of them.

The recorded IR (gas and liquid phases) and Raman (liquid phase) spectra in this work for ITMS are shown in Fig. 3. In

Table 3 Refined and calculated geometric parameters with *ab initio* and DFT values and restraints for ITMS (distances in pm, angles in °) from the SARACEN GED study[a]

Parameter	Description	GED (r_{h1})	MP2/GEN[b] (r_e)	MP2/6-311G** (r_e)	B3LYP/LanL2DZdp	Restraint
P_1	rC–H	109.2(3)	109.5	109.5	109.9	—
P_2	rSi–C	187.3(1)	187.0	186.8	187.6	—
P_3	rSi–I	248.6(2)	248.5	249.9	250.5	—
P_4	∠Si–C–H	111.0(3)	110.8	110.5	110.8	110.8(3)
P_5	∠I–Si–C	106.6(1)	107.3	107.5	107.3	—
P_6	Me tilt	0.4(8)	—	—	—	1.0(10)

[a] Figures in parentheses are the estimated standard deviations of the last digits. See text for parameter definitions. [b] 6-311+G* on H, C and Si, SDB-cc-pVTZ on I.

Table 4 Experimental and scaled frequencies (in cm^{-1}) for ITMS, with the description of each normal mode, proposal of assignment and comparison with results from previous work[a]

	Experimental			Scaled DFT (B3LYP)					
	IR gas	IR liquid	Raman liquid	LanL2DZ	LanL2DZdp	6-311G**	Bürger[14] [b]	Goubeau and Sommer[13] [c]	Description
A_1									
ν_1	2967 s	2959 s	2959 s	2968	2961	2960	2973	2973	$\nu_{as}CH$
ν_2	2906 m	2897 m	2896 vs, p	2880	2892	2893	2913	2902	$\nu_{s}CH$
ν_3	1420 sh	—	—	1415	1416	1417	1415	1404	$\delta_{as}CH_3$
ν_4	1267 sh	1252 vs	1263 vw, p	1266	1263	1264	1261	1255	$\delta_{s}CH_3$
ν_5	851 vs, br	849 vs, br	850 w, p	850	849	850	852	845	ρCH_3
ν_6	627 m	623 s	624 m, p	625	627	628	628	627	νSiC
ν_7	—	—	326 m, p	325	326	326	333^{+}	331	$\nu SiI + \delta_{s}SiC_3$
ν_8	—	—	194 m, p	195	193	192	—	198	$\delta_{s}SiC_3 + \nu SiI + \rho CH_3$
A_2									
ν_9	—	—	—	2986	2978	2978	—	—	$\nu_{as}CH$
ν_{10}	—	—	—	1391	1391	1390	—	—	$\delta_{as}CH_3$
ν_{11}	—	—	—	676	677	674	—	—	ρCH_3
ν_{12}	—	—	—	101	135	136	—	—	τ SiC
E									
ν_{13}	2980 sh	2972 s	2973 s, dp	2987	2979	2979	2973	2973	$\nu_{as}CH$
ν_{14}	2967 s	2959 s	2959 s, dp	2966	2959	2959			$\nu_{as}CH$
ν_{15}	2906 m	2897 m	2896 vs	2878	2890	2891	2913	2902	$\nu_{s}CH$
ν_{16}	1413 m	1410 m	1413 w, dp	1404	1404	1404	1415	1404	$\delta_{as}CH_3$
ν_{17}	1404 sh	1393 sh	—	1401	1401	1400			$\delta_{as}CH_3$
ν_{18}	1259 s	1252 vs	1252 vw, dp	1253	1254	1254	1261	1255	$\delta_{s}CH_3$
ν_{19}	851 vs, br	849 vs, br	850 w	858	853	855	852	845	$\rho CH_3 + \nu SiC$
ν_{20}	760 m	760 s	759 w, dp	756	759	759	763	761	$\rho CH_3 + \nu SiC$
ν_{21}	698 w	698 m	698 w, dp	691	692	689	703	704	$\rho CH_3 + \nu SiC$
ν_{22}	—	—	230 m, dp	228	229	228	233^{+}	231	$\delta_{as}SiC_3 + \rho CH_3$
ν_{23}	—	—	161 m, dp	161	161	158	163^{+}	164	$\rho SiC_3 + \delta_{as}SiC_3$
ν_{24}	—	—	—	131	153	155	—	—	τ SiC
rmsd/cm^{-1}				8.26	4.09	4.38			

[a] Abbreviations: vs: very strong, s: strong, m: medium, w: weak, vw: very weak, br: broad, sh: shoulder, p: polarised band, dp: depolarised band. [b] Experimental data from the IR spectrum of the gas phase, except: $^{+}$from the IR spectrum of the liquid phase. [c] Experimental data from the Raman spectrum of the liquid phase.

Table 4, experimental and scaled (after refinement of scale factors) frequencies are reported, along with a qualitative description of each normal mode of the molecule based on the potential energy distribution matrix (PEDM). The assignments by previous authors[13,14] are also presented in Table 4, for comparison.

In addition to the bands corresponding to the vibrations of ITMS that will be discussed below, we have observed two bands in the IR of the liquid phase, specifically at 1055 cm^{-1} (1074 cm^{-1} in the IR of the gas phase) and 656 cm^{-1}, that cannot be assigned to any vibration of the ITMS molecule. These are due to the presence of hexamethyldisiloxane (HMDSO) in the sample, which is an impurity that appears as a product of the hydrolysis and later condensation of two trimethylsilylhalide units in presence of atmospheric water.[36] The peak at 1055 cm^{-1} belongs to the SiOSi stretching normal mode and the one at 656 cm^{-1} is described as the SiC stretching normal mode of the HMDSO molecule.[37]

Discussion

Molecular structure

The molecular structure of iodotrimethylsilane has been probed using various structural and spectroscopic methods. The gaseous structure of ITMS has been investigated using diffraction techniques in combination with *ab initio* methods. One discussion point raised by the *ab initio* investigation was the substantially different values returned for the Si–I bond length by the two highest-level calculations. The all-electron 6-311G** basis set returned a value of 249.9 pm, whilst the use of a pseudopotential on iodine reduced this length to 248.5 pm. This parameter is one that is very well defined in the GED experiment. Examination of Fig. 2 reveals that there is only one, very large, peak in the radial distribution curve at $\sim$250 pm, confirming that the internuclear distance between the two atoms causing that peak should be well determined. From Table 3, it can be seen that the experimental (r_{h1}) Si–I distance was 248.6(2) pm. The anharmonic correction to the experimental value was 0.4 pm, giving an r_e value of 248.2 pm for the Si–I distance. The anharmonic correction (r_{h1} or r_e) was calculated from 3/2*a*u^2 (where a is 1.405 as taken from the shrink output file, and u is the RMS amplitude of vibration). This can then be directly compared with the calculated values (MP2/6-311+G*//SDB-cc-pVTZ 248.5 pm; MP2/6-311G* 249.9 pm) and in this respect and others the experimental structure agrees very well with the results of the *ab initio* calculation where the pseudopotential was used. It should also be noted that, on the workstation used, the calculation with the pseudopotential was eight times quicker than the all-electron calculation. Whilst for a molecule of this size processor time is not an issue, for larger molecules it is, and it has

been shown that excellent results can be obtained with the use of a pseudopotential, for a fraction of the computer time. The microwave stucture reported by Rexroad *et al* indicated a Si–I bond length of 246(2) pm.[12] When compared to the *ab initio* and GED structures this distance seems short, although the error almost encompasses the newly determined values. Many structural assumptions were made in the original microwave study, and perhaps a revised investigation would be prudent in light of new information about the structure of ITMS.

When comparing the structural parameters for $SiMe_3X$, where X = H, F, Cl, Br and I, the results of the MP2(fc)/6-311G** calculations will be used at all times. From Table 2, it can be seen that both ∠ Si–C–Hα and ∠ Si–C–Hβ decrease in size from H > F > Cl > Br > I, whilst the difference between these two angles increases from 0.4° for X = H, to 1.3° for X = I. To gauge the cause of these effects the ∠ Hα–C–Hβ and ∠ Hβ–C–Hβ angles were examined. Both were found to be effectively the same value throughout the series (107.8–108.2°), indicating that the change in ∠ Si–C–H is due to a tilt of the methyl groups away from the increasingly bulky halogen atom, rather than distortion within the methyl groups themselves. This effect was accounted for in the GED model by the inclusion of a methyl tilt parameter.

The X–Si–C angle is larger for X = H than for all the other substituents (108.8° compared to ~107.4°). This correlates with the increase in the Si–X bond lengths, with the repulsion from atom X decreasing as the bond length increases. There can also be an effect due to electronegativity, as X attracts electrons, so the angles at silicon change. The Si–C bond lengths also show a significant shortening from 188.0 pm to

Table 5 Comparison between experimental and scaled frequencies (in cm^{-1}) for TMS, FTMS, CTMS, BTMS and ITMS

TMS		FTMS		CTMS		BTMS		ITMS		
Expt.[c]	Scaled.[a]	Expt.[d]	Scaled[a]	Expt.[e]	Scaled[a]	Expt.[f]	Scaled[a]	Expt.[g]	Scaled[b]	Description
A_1										
2964	2969	2967	2970	2963	2967	2961	2964	2959	2960	$\nu_{as}CH$
2900	2900	2906	2902	2902	2898	2900	2893	2897	2893	$\nu_{s}CH$
2119	2119	—	—	—	—	—	—	—	—	νSiH
1428^{+}	1421	1425*	1426	1421	1424	1419	1421	1420^{x}	1417	$\delta_{as}CH_3$
1263	1262	1268	1260	1275	1266	1270	1264	1252	1264	$\delta_{s}CH_3$
—	—	895	910	—	—	—	—	—	—	$\nu SiF + \rho CH_3$
853	857	—	—	848	851	848	853	849	850	ρCH_3
—	—	770	760	—	—	—	—	—	—	$\nu SiF + \rho CH_3$
624	622	618	608	636	640	631	637	623	628	νSiC
—	—	—	—	471	470	—	—	—	—	$\nu SiCl$
—	—	—	—	—	—	376	376	—	—	$\nu SiBr + \rho SiC_3$
—	—	—	—	—	—	—	—	326^{xx}	326	$\nu SiI + \rho SiC_3$
252	251	242	237	—	—	—	—	—	—	$\delta_{s}SiC_3 + \rho CH_3$
—	—	—	—	228	227	$212^{\$}$	210	—	—	$\delta_{s}SiC_3$
—	—	—	—	—	—	—	—	194^{xx}	192	$\delta_{s}SiC_3 + \nu SiI + \rho CH_3$
A_2										
—	2967	—	2974	—	2979	—	2980	—	2978	$\nu_{as}CH$
—	1403	—	1403	—	1400	—	1398	—	1390	$\delta_{as}CH_3$
—	650	—	660	—	660	—	659	—	674	ρCH_3
—	143	—	133	$157^{\#}$	156	—	156	—	136	τ SiC
E										
2975^{+}	2972	2967	2976	2970	2980	2974	2981	2972	2979	$\nu_{as}CH$
2964	2967	2967	2967	2963	2964	2961	2961	2959	2959	$\nu_{as}CH$
2900	2899	2906	2900	2902	2896	2900	2893	2897	2891	$\nu_{s}CH$
1411	1414	1415	1415	1414	1413	1412	1410	1410	1404	$\delta_{as}CH_3$
—	1405	1410	1410	—	1407	1404	1404	1393	1400	$\delta_{as}CH_3$
1253	1254	1254	1254	1255	1259	1254	1257	1252	1254	$\delta_{s}CH_3$
905	901	—	—	—	—	—	—	—	—	$\rho SiC_3 + \rho CH_3$
—	—	852	870	848	854	848	857	849	855	$\rho CH_3 + \nu SiC$
831	829	—	—	—	—	—	—	—	—	ρCH_3
—	—	756	760	760	760	760	758	760	759	$\rho CH_3 + \nu SiC$
711	712	—	—	—	—	—	—	—	—	νSiC
—	—	—	—	696	686	—	—	—	—	ρCH_3
—	—	695	686	—	—	698	684	698	689	$\rho CH_3 + \nu SiC$
616^{++}	594	—	—	—	—	—	—	—	—	$\rho CH_3 + \rho SiC_3$
—	—	291	290	—	—	—	—	—	—	$\rho SiC_3 + \delta_{as}SiC_3$
216	216	—	—	$243^{\#\#}$	246	—	—	230^{xx}	228	$\delta_{as}SiC_3 + \rho CH_3$
—	—	—	—	—	—	$235^{\$}$	232	—	—	$\delta_{as}SiC_3 + \rho SiC_3$
—	—	205	197	$187^{\#\#}$	183	$174^{\$}$	170	161^{xx}	158	$\rho SiC_3 + \delta_{as}SiC_3$
—	155	—	150	$170^{\#}$	171	—	174	—	155	τ SiC

[a] Scaled B3LYP/6-31G* (taken from ref. 11). [b] Scaled B3LYP/6-311G**. [c] Experimental data from the Raman spectrum (liquid phase) except: $^{+}$IR (gas phase), $^{++}$ IR (solid phase). [d] Experimental data from the Raman spectrum (liquid phase) except: * IR (gas phase). [e] Experimental data from the IR spectrum (liquid phase) except: # INS spectrum, ## Raman (liquid phase). [f] Experimental data from the IR spectrum (liquid phase) except: $^{\$}$Raman (liquid phase.) [g] Experimental data from the IR spectrum (liquid phase) except: ^{x} IR (gas phase), ^{xx} Raman (liquid phase).

186.4 pm on going from X = H to X = F. This is not unusual in this type of silicon compound, but may initially seem counterintuitive as F is very electron-withdrawing and the adjacent bonds would be expected to lengthen, not shorten. However, examination of the Mulliken charges on Si and C indicate that the Si is very positively charged when X = F compared to X = H (1.436 compared to 1.086). Thus the electronegative F atom makes the Si atom more positively charged, which in turn strongly attracts the overall negatively charged methyl groups. Hence the Si–C bond is actually shorter, rather than longer as initially expected.

Vibrational spectra

In the discussion, and unless otherwise stated, the references will be to the vibrational bands observed in the IR spectrum of the liquid phase and the theoretical results at B3LYP/6-311G** level. For the sake of clarity, the analysis of the vibrational spectra of ITMS has been divided into sections. The discussion will focus on the less reliable parts of the vibrational assignments appearing in the literature.[13,14] The trends followed in this paper were established in previous work,[9–11] where a set of unified criteria for the vibrational analysis of this family of compounds was proposed.

CH_3 stretching modes. In the IR spectrum of the liquid phase two strong bands at 2972 cm^{-1} (shoulder in the IR of the gas phase at 2980 cm^{-1} and a depolarised band at 2973 cm^{-1} in the Raman of the liquid phase) and 2959 cm^{-1} (2967 cm^{-1} in the IR of the gas and a depolarised band at 2959 cm^{-1} in the Raman spectrum) are observed. Calculations predict the presence of four vibrational bands, *i.e.* $1A_1 + 1A_2 + 2E$, which, in agreement with the results of the scaling process, have been assigned as follows. The band at 2972 cm^{-1} was assigned to $\nu_{13}(E)$, and that at 2959 cm^{-1} to $\nu_1(A_1)$ and $\nu_{14}(E)$, which were calculated to be very close to each other. The frequency of the ν_9 (A_2) normal mode is proposed to be 2978 cm^{-1}.

These proposals contrast with those of previous work,[13,14] where only one band was observed in this region, at 2973 cm^{-1}, assigned to the three asymmetric stretching modes expected to be active in IR and Raman, namely ν_1, ν_{13} and ν_{14}. In addition, these new assignments are in perfect agreement with the results obtained for the rest of the molecules of the series.[9–11] In fact, in [ref. 11] it was pointed out that the splitting of the asymmetric CH_3 stretching modes observed for the family of compounds (Me_3SiX, X = H, F, Cl or Br) could be related to the differences between the lengths of the CH_α and CH_β bonds (Fig. 1). From the theoretical values (Table 2), these differences seem to increase with the size of the X atoms, including the iodine atom. In agreement with this, the values of the scaled frequencies of these normal modes follow the same tendency, with the differences between them increasing from H to I. The results of the vibrational assignments for all the derivatives of the series are presented in Table 5.

The symmetric modes $\nu_2(A_1)$ and $\nu_{15}(E)$ are both assigned to the observed band at 2897 cm^{-1} in the IR spectrum of the liquid [2906 cm^{-1} (gas-phase); 2896 cm^{-1}, polarised (Raman)], in agreement with the theoretical values after scaling and with previous work.

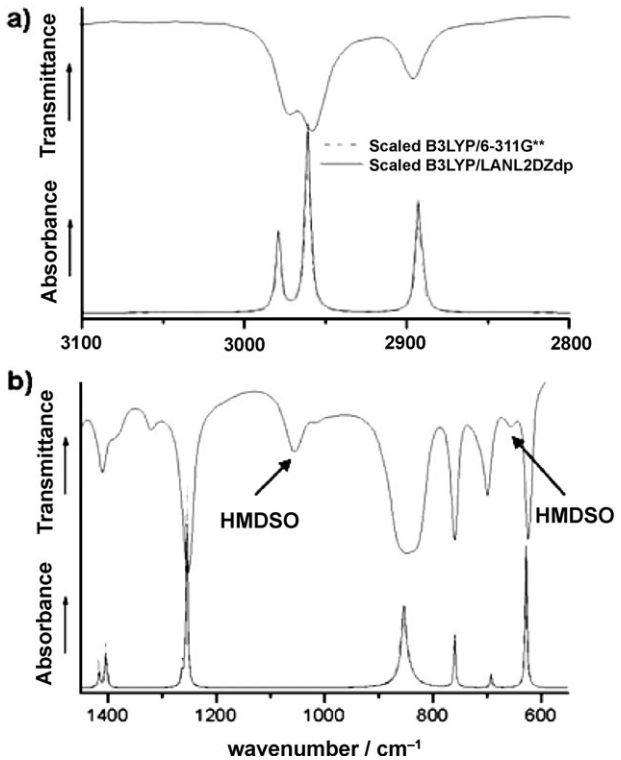

Fig. 4 Comparison of absorbance calculated at the B3LYP/LanL2DZdp and B3LYP/6-311G** levels *vs.* experimental (transmittance) IR spectrum (liquid phase) of ITMS showing the regions (a) between 3100 and 2850 cm^{-1} and (b) between 1450 and 550 cm^{-1}.

The theoretical calculations using B3LYP/LanL2DZ, even after scaling the force field, reproduce this spectral region poorly. However, the introduction of polarisation and diffuse functions to the basis set for the heavy atoms (LanL2DZdp) greatly improves the spectral profile calculated in this zone. This is shown in Fig. S2,† where the IR spectrum of the liquid phase (upper, in transmittance) is compared with the spectrum calculated at the B3LYP/LanL2DZ and B3LYP/LanL2DZdp levels (lower, in absorbance). Furthermore, as can be seen in Fig. 4a, the results at both B3LYP/LanL2DZdp and B3LYP/6-311G** levels give very good agreement for these modes.

CH_3 deformation modes. Four normal modes of ITMS belonging to the asymmetric methyl deformations of the molecule are expected to appear in the vibrational spectra. In the IR of the liquid phase only two bands can be distinguished, one at 1410 cm^{-1} [1413 cm^{-1} (IR, gas-phase), 1413 cm^{-1}, depolarised (Raman)] and the second at 1393 cm^{-1} [1404 cm^{-1}, shoulder (gas phase)]. However, one more band in the gas-phase IR can be observed at 1420 cm^{-1}. Thus the band observed at 1420 cm^{-1} (gas) can be assigned to $\nu_3(A_1)$, and the bands of the IR (liquid) at 1413 and 1393 cm^{-1} to the normal modes ν_{16} and ν_{17} (both of E symmetry) in accordance with theoretical calculations.

To complete the description of the high-frequency zone of this spectral region, the $\nu_{10}(A_2)$ normal mode, Raman- and IR-inactive, is predicted to be at 1390 cm^{-1}, after refinement of the scale factors. Previous work[13,14] reported only one

Table 6 Combination bands and overtones observed in the vibrational spectra of TMS, FTMS, CTMS, BTMS and ITMS, and their descriptions

TMS IR gas	FTMS IR gas	IR solid	CTMS IR gas	IR liquid	BTMS IR gas	IR liquid	ITMS IR gas	IR liquid	Description
2827	—	—	—	—	—	—	—	—	$2\nu_{16}$
—	—	—	—	2790	—	—	—	—	$\nu_{14} - \nu_{24}$
—	—	—	—	—	—	—	—	2779	$2\nu_{10}$
—	—	—	—	—	—	—	—	2662	$\nu_{16} + \nu_{18}$
—	—	—	—	2498	—	—	—	—	$\nu_1 - \nu_7$
—	—	—	2118	2112	—	—	—	2112	$\nu_{16} + \nu_{21}$
—	—	—	2022	2016	—	2012	2015	2012	$\nu_{18} + \nu_{20}$
1965	—	—	1957	1951	—	1948	—	—	$\nu_{18} + \nu_{21}$
—	—	—	—	—	1588	—	—	—	$\nu_{16} + \nu_{23}$
1883	—	—	—	—	—	—	—	—	$\nu_5 + \nu_7$
—	—	—	1899	1890	—	—	—	—	$\nu_3 + \nu_7$
1467	—	—	—	—	—	—	—	—	$\nu_{18} + \nu_{23}$
—	1450	1447	1456	1454	1453	1453	1454	1456	$\nu_{20} + \nu_{21}$
1330	—	—	1335	1335	1327	—	1322	1319	$2\nu_{11}$

vibrational band for the three active modes of asymmetric methyl deformations.

For the symmetric methyl deformation modes, only one very strong band at 1252 cm^{-1} can be observed in the IR of the liquid phase, while in the IR of the gas phase it is possible to distinguish one strong band at 1259 cm^{-1} with a shoulder at 1267 cm^{-1} [1252 cm^{-1} depolarised and 1263 cm^{-1} polarised, respectively, (Raman)]. These experimental observations allowed the band at the higher frequency to be assigned to $\nu_4(A_1)$ and the band at lower frequency to $\nu_{18}(E)$, in accordance with the values calculated after refinement of the scale factors. Previously,[13,14] only one band was observed for these two modes, so this new description for this spectral zone is also more complete than before.

Skeletal modes. The so-called skeletal modes of this molecule appear below 900 cm^{-1}. The new spectral records reported in this paper do not show any more bands than those reported earlier.[13,14] Our assignment for this region therefore effectively agrees with those previously proposed by Goubeau and Sommer[13] and Bürger.[14] Theoretical calculations confirm this proposal, and allow the prediction of values for the inactive (A_2) modes ν_{11} at 674 cm^{-1} and ν_{12} at 136 cm^{-1}, described as methyl rocking and SiC bond torsion normal modes, respectively. In addition, a theoretical value for the unobserved torsional mode $\nu_{24}(E)$ at 155 cm^{-1} is proposed.

Fig. 4b shows the IR spectrum from 1450 to 550 cm^{-1} of the liquid phase (upper) and those calculated at B3LYP/LanL2DZdp and B3LYP/6-311G** levels (lower). It can be seen that there is good agreement between the experimental and theoretical results, corroborated by the low values of the root-mean-square (rms) deviations shown in Table 4. However, while the whole spectral profiles at the B3LYP/LanL2DZdp and B3LYP/6-311G** levels are almost identical, the B3LYP/LanL2DZ level fails mainly when reproducing the CH stretching region and, consequently, the rms deviation is higher. The final values of the scale factors (after refinement by the SQM method) associated with the natural coordinates defined for ITMS are reported in Table S7, at the three levels of calculation used.†

In Table 5, the vibrational assignments proposed in this paper for all the molecules of the series are summarised. When comparing the results for the complete set of molecules, only small differences are observed between the experimental spectra, these differences being slightly larger in the cases of TMS and FTMS. The predicted values for all the A_2 inactive normal modes and the frequencies calculated for the Si–C torsional modes of E symmetry (which are unobserved) have similar values for all the molecules of the series, even taking into account that a basis set other than 6-31G* was used for ITMS. In addition, all the observed bands not related to fundamental vibrations have been assigned to combinations and overtones. These, along with those observed in the cases of TMS, FTMS, CTMS and BTMS, are presented in Table 6 and good agreement is observed, even for these bands.

Conclusions

A complete investigation of the molecular structure of iodotrimethylsilane has been carried out in the gas phase by gas electron diffraction complemented by theoretical methods. The experimental and theoretical structures agree that ITMS possesses C_{3v} symmetry. A pseudopotential was required to describe the iodine atom, and the SDB-cc-pVTZ basis set and ECP was found to provide the best mix of accuracy and efficiency.

New IR and Raman spectra of ITMS have been recorded, allowing improved vibrational assignment for the title molecule compared with the results found in the literature,[13,14] particularly for the description of the asymmetric C–H stretching and methyl deformation spectral regions. The modes $\nu_3(A_1)$, ν_{13}, ν_{16} and ν_{17} (all E species) have all been reassigned. New calculated values are given for the A_2 (Raman- and IR-inactive) normal modes and for the ν_{24} (E) Si–C torsional mode.

In the vibrational analysis, the LanL2DZdp-ECP and 6-311G** basis sets gave values very close to the experimental frequencies after the refinement of the scale factors at the DFT level. They also gave an adequate description of the spectral profile of the molecule. The results obtained with the LanL2DZ basis set are worse, mainly in the region where the C–H stretching normal modes appear. Finally, all the experimental and scaled frequencies for the family of

compounds are compared, showing very good agreement between them.

Acknowledgements

MM thanks the Fundación Ramón Areces for a PhD grant supporting this work. ABA thanks CONICET (Consejo Nacional de Investigaciones Científicas y Técnicas) and CIUNT (Consejo de Investigaciones de la Universidad Nacional de Tucumán) for research grants, and the Junta de Andalucía for their financial support for her stay in Jaén. MM, ABA, FPU, and JJLG thank Dr Tom Sundius for allowing the use of MOLVIB and Francisco Hermoso for help recording the spectra. SLH, HER and DWHR thank the EPSRC for funding the electron diffraction research (GR/N22407).

References

1 C. J. Brinker and G. W. Scherer, *Sol-Gel Science: The Physics and Chemistry of Sol-Gel Processing*, Academic Press, San Diego, CA, 1989.
2 A. H. Schmidt, *Aldrichimica Acta*, 1981, **14**, 31.
3 A. K. Banerjee, *J. Sci. Ind. Res.*, 1982, **41**, 699.
4 A. Casnati, A. Arduini, E. Ghidini, A. Pochini and R. Ungaro, *Tetrahedron*, 1991, **47**, 2221.
5 M. G. Voronkov and E. I. Dubinskaya, *J. Organomet. Chem.*, 1991, **410**, 13.
6 A. Hosomi and K. Miura, in *Lewis Acid Reagents. A Practical Approach*, ed. H. Yamamoto, Oxford University Press, Oxford, 1999, p. 159.
7 P. Y. Renard, P. Vayron and C. Mioskowski, *Org. Lett.*, 2003, **5**, 1661.
8 G. Sabitha, G. S. K. K. Reddy, Ch. S. Reddy and Y. J. S. Srinivas, *Tetrahedron Lett.*, 2003, **44**, 4129.
9 M. Montejo, F. Partal Ureña, F. Márquez, I. S. Ignatyev and J. J. López González, *J. Mol. Struct.*, 2005, **744–747**, 331.
10 M. Montejo, F. Partal Ureña, F. Márquez, I. S. Ignatyev and J. J. López González, *Spectrochim. Acta, Part A*, 2005, **62**, 293.
11 M. Montejo, F. Partal Ureña, F. Márquez, J. J. López and González, *Spectrochim. Acta, Part A*, DOI: 10.1016/j.saa.2005.04.003.
12 H. N. Rexroad, D. W. Howgate, R. C. Gunton and J. F. Ollom, *J. Chem. Phys.*, 1956, **24**, 625.
13 J. Goubeau and H. Sommer, *Z. Anorg. Allg. Chem.*, 1957, **289**, 1.
14 H. Bürger, *Spectrochim. Acta, Part A*, 1968, **24**, 2015.
15 C. M. Huntley, G. S. Laurenson and D. W. H. Rankin, *J. Chem. Soc., Dalton Trans.*, 1980, 954.
16 H. Fleischer, D. A. Wann, S. L. Hinchley, K. B. Borisenko, J. R. Lewis, R. J. Mawhorter, H. E. Robertson and D. W. H. Rankin, *Dalton Trans.*, 2005, 3221.
17 S. L. Hinchley, H. E. Robertson, K. B. Borisenko, A. R. Turner, B. F. Johnston, D. W. H. Rankin, M. Ahmadian, J. N. Jones and A. H. Cowley, *Dalton Trans.*, 2004, 2469.
18 A. W. Ross, M. Fink and R. Hilderbrandt, in *International Tables for Crystallography Volume C*, ed. A. J. C. Wilson, Kluwer Academic Publishers, Dordrecht, Netherlands, 1992, p. 245.
19 M. J. Frisch, G. W. Trucks, H. B. Schlegel, G. E. Scuseria, M. A. Robb, J. R. Cheeseman, J. A. Montgomery Jr, T. Vreven, K. N. Kudin, J. C. Burant, J. M. Millam, S. S. Iyengar, J. Tomasi, V. Barone, B. Mennucci, M. Cossi, G. Scalmani, N. Rega, G. A. Petersson, H. Nakatsuji, M. Hada, M. Ehara, K. Toyota, R. Fukuda, J. Hasegawa, M. Ishida, T. Nakajima, Y. Honda, O. Kitao, H. Nakai, M. Klene, X. Li, J. E. Knox, H. P. Hratchian, J. B. Cross, C. Adamo, J. Jaramillo, R. Gomperts, R. E. Stratmann, O. Yazyev, A. J. Austin, R. Cammi, C. Pomelli, J. W. Ochterski, P. Y. Ayala, K. Morokuma, G. A. Voth, P. Salvador, J. J. Dannenberg, V. G. Zakrzewski, S. Dapprich, A. D. Daniels, M. C. Strain, O. Farkas, D. K. Malick, A. D. Rabuck, K. Raghavachari, J. B. Foresman, J. V. Ortiz, Q. Cui, A. G. Baboul, S. Clifford, J. Cioslowski, B. B. Stefanov, G. Liu, A. Liashenko, P. Piskorz, I. Komaromi, R. L. Martin, D. J. Fox, T. Keith, M. A. Al-Laham, C. Y. Peng, A. Nanayakkara, M. Challacombe, P. M. W. Gill, B. Johnson, W. Chen, M. W. Wong, C. Gonzalez and J. A. Pople, *GAUSSIAN 03 (Revision C.01)*, Gaussian, Inc., Wallingford, CT, 2004.
20 (*a*) D. R. Hartree, *Proc. Cambridge Philos. Soc.*, 1928, **24**, 89; (*b*) V. Fock, *Z. Phys.*, 1930, **61**, 126; (*c*) V. Fock, *Z. Phys.*, 1930, **62**, 795.
21 (*a*) J. S. Binkley, J. A. Pople and W. J. Hehre, *J. Am. Chem. Soc.*, 1980, **102**, 939; (*b*) M. S. Gordon, J. S. Binkley, J. A. Pople, W. J. Pietro and W. J. Hehre, *J. Am. Chem. Soc.*, 1982, **104**, 2797; (*c*) W. J. Pietro, M. M. Francl, W. J. Hehre, D. J. Defrees, J. A. Pople and J. S. Binkley, *J. Am. Chem. Soc.*, 1982, **104**, 5039; (*d*) K. D. Dobbs and W. J. Hehre, *J. Comput. Chem.*, 1986, **7**, 359; (*e*) K. D. Dobbs and W. J. Hehre, *J. Comput. Chem.*, 1987, **8**, 861; (*f*) K. D. Dobbs and W. J. Hehre, *J. Comput. Chem.*, 1987, **8**, 880.
22 (*a*) M. N. Glukhovtsev, A. Pross, M. P. McGrath and L. Radom, *J. Chem. Phys.*, 1995, **103**, 1878; (*b*) A. D. McLean and G. S. Chandler, *J. Chem. Phys.*, 1980, **72**, 5639; (*c*) R. Krishnan, J. S. Binkley, R. Seeger and J. A. Pople, *J. Chem. Phys.*, 1980, **72**, 650.
23 (*a*) J. M. L. Martin and A. Sundermann, *J. Chem. Phys.*, 2001, **114**, 3408; (*b*) A. Bergner, M. Dolg, W. Kuechle, H. Stoll and H. Preuss, *Mol. Phys.*, 1993, **80**, 1431.
24 (*a*) R. Ditchfield, W. J. Hehre and J. A. Pople, *J. Chem. Phys.*, 1971, **54**, 724; (*b*) W. J. Hehre, R. Ditchfield and J. A. Pople, *J. Chem. Phys.*, 1972, **56**, 2257; (*c*) P. C. Hariharan and J. A. Pople, *Mol. Phys.*, 1974, **27**, 209; (*d*) M. S. Gordon, *Chem. Phys. Lett.*, 1980, **76**, 163; (*e*) P. C. Hariharan and J. A. Pople, *Theor. Chim. Acta*, 1973, **28**, 213; (*f*) J.-P. Blaudeau, M. P. McGrath, L. A. Curtiss and L. Radom, *J. Chem. Phys.*, 1997, **107**, 5016; (*g*) M. M. Francl, W. J. Pietro, W. J. Hehre, J. S. Binkley, D. J. DeFrees, J. A. Pople and M. S. Gordon, *J. Chem. Phys.*, 1982, **77**, 3654; (*h*) R. C. Binning Jr. and L. A. Curtiss, *J. Comput. Chem.*, 1990, **11**, 1206; (*i*) V. A. Rassolov, J. A. Pople, M. A. Ratner and T. L. Windus, *J. Chem. Phys.*, 1998, **109**, 1223; (*j*) V. A. Rassolov, M. A. Ratner, J. A. Pople, P. C. Redfern and L. A. Curtiss, *J. Comput. Chem.*, 2001, **22**, 976.
25 C. Møller and M. S. Plesset, *Phys. Rev.*, 1934, **46**, 618.
26 A. D. J. Becke, *J. Chem. Phys.*, 1993, **98**, 5648.
27 C. Lee, W. Yang and R. G. Parr, *Phys. Rev. B*, 1988, **37**, 785.
28 J. V. Ortiz, P. J. Hay and R. L. Martin, *J. Am. Chem. Soc.*, 1992, **114**, 2736.
29 C. E. Check, T. O. Faust, J. M. Bailey, B. J. Wright, T. M. Gilbert and L. S. Sunderlin, *J. Phys. Chem. A*, 2001, **105**, 8111.
30 G. Fogarasi and P. Pulay, in *Vibrational Spectra and Structure*, ed. James E. Durig, Elsevier, Amsterdam, vol. 14, 1985, p. 125.
31 T. Sundius, *J. Mol. Struct.*, 1990, **218**, 321.
32 T. Sundius, *Vib. Spectrosc.*, 2002, **29**, 89.
33 (*a*) G. Rauhut and P. Pulay, *J. Phys. Chem.*, 1995, **99**, 3093; (*b*) G. Rauhut and P. Pulay, *J. Phys. Chem.*, 1995, **99**, 14572.
34 V. A. Sipachev, *J. Mol. Struct. (THEOCHEM)*, 1985, **121**, 143.
35 (*a*) P. T. Brain, C. A. Morrison, S. Parsons and D. W. H. Rankin, *J. Chem. Soc., Dalton Trans.*, 1996, 4589; (*b*) A. J. Blake, P. T. Brain, H. McNab, J. Miller, C. A. Morrison, S. Parsons, D. W. H. Rankin, H. E. Robertson and B. A. Smart, *J. Phys. Chem.*, 1996, **100**, 12280; (*c*) N. W. Mitzel and D. W. H. Rankin, *Dalton Trans.*, 2003, 3650.
36 Y. S. Li and K. Le, *Spectrochim. Acta, Part A*, 2004, **60**, 927.
37 A. L. Lazarev, I. S. Ignatyev and T. F. Tenisheva, *The Chemistry of Molecules Containing SiO Bonds*, Nauka Publishers, St Petersburg, 1980.